

Delong Xie*, Haiqing Qin, Feng Lin, Xiaoyi Pan, Chao Chen, Leyin Xiao, Jiarong Chen, Peicheng Mo

Guangxi Key Laboratory of Superhard Materials,
Chinese National Engineering Research Center for Special Mineral
Materials, China Nonferrous Metal (Guilin) Geology
and Mining Co., Ltd, Guilin, China

*xiedelonghn@foxmail.com

Microstructures and properties of Fe–Co–Cu pre-alloyed powder for geological diamond bits

For geological diamond bits Fe–Co–Cu alloys are the new generation of metal matrix. In this paper, the Fe–Co–Cu pre-alloys with various chemical compositions were synthesized using the co-precipitation method, which were subsequently sintered at different temperatures. The structural, thermal and properties of the powders and its sintered materials were characterized by various techniques. X-ray diffraction studies indicated that solid solutions were formed for the alloys during co-precipitation process. Microstructures of these pre-alloyed powders exhibited that the sintering process was facilitated by the irregular shapes, interconnected fine particles as well as the large surface areas. The thermal effects of the pre-alloyed powders were explored by differential scanning calorimetry. The optimal sintering temperature for each pre-alloyed powder was determined by the mechanical analysis. Scanning electron microscopic results show that the composition ratio of Fe and Cu had a significant impact on the microstructures of the sintered materials, and the 65%Fe–20%Cu–15%Co alloy reached the best surface coverage over the diamond bits. The drilling performances for various pre-alloyed powders were verified by micro-drilling experiments. Those results suggested that the 65%Fe–20%Cu–15%Co alloy exhibited the optimal performance for application in geological diamond drilling bits.

Keywords: *pre-alloyed powder, sintering, co-precipitation method, geological diamond bit.*

INTRODUCTION

In powder metallurgy processed geological diamond bits, the matrix usually are obtained by mixtures of the elemental powders [1]. The inhomogeneous component can result in composition of matrix segregating easily, so properties of the diamond bits are largely influenced. In order to overcome this limitation and improve the bits' properties, more attention is paid to the alloying powder [2]. Nowadays, the majority of the diamond tools such as saw blades, bits and wire saw employ pre-alloyed powders as bonding metal matrix [3]. A lot of work has been devoted to the study of the properties of composite diamond-containing materials based on metal matrices containing iron, cobalt, copper, etc., sintered by the methods of powder metallurgy. The most significant scientific and practical results on the formation of a structure with improved mechanical characteristics of such composites were obtained in [4–8]. The properties of these

composites are determined by the composition, structure and morphology, which, in turn, depend on the properties of the constituents, methods and modes of sintering. Some important properties of composites vary depending on the force parameters of rock failure [9], contact temperatures [10–12], stress–strain state of the matrix [13, 14], as well as placement of composites on the tool working surface [15].

At present, researches of pre-alloyed powder focus on iron–cobalt–copper (Fe–Co–Cu) based system. Co presents good chemical compatibility with diamond at the sintering processing, ideal mechanic properties, and fine diamond retention. Co powders are widely employed in the manufacture of metal matrix diamond tools [16].

Nevertheless, the challenges of the Co element are associated with its high price and limited resource. Meanwhile, due to the high toxicity of cobalt, the metal dust during the producing processes is particularly hazardous [17]. Therefore, other metals like Fe are proposed to replace cobalt. Both iron and cobalt are group VIII elements, hence they have some common proprieties. Fe is so inexpensive that it has advantages of economic benefit. More and more researches focus on using Fe to substitute Co. Copper has exceptional moldability, low fusing point, being easy to form alloy with other metals. Nearly all diamond tools use copper element.

Sintering temperatures of current Fe–Co–Cu systems commonly exceed 900 °C, which causes thermal damages to the diamonds because graphitization temperature of diamonds is under 900 °C. In addition, the mechanical properties of Fe–Co–Cu systems such as hardness and strength are the main origins for selecting a metal matrix for bonding diamonds in impregnated diamond tools [18–19], but the selection of bonding metal also depends on the abrasiveness and hardness of the material to be processed. Accordingly it should be doubted to only adopt the mechanical properties to judge the performance of metal bond.

This paper is dedicated to study the microstructure of the Fe–Co–Cu pre-alloyed powder, mechanical properties of the systems of (25–45–65)Fe–15Co–(60–40–20)Cu* at different sintering temperatures and the application of drilling medium to hard formation (drill ability 7). It is worth to mention that for different Fe–Co–Cu compositions the suitable sintering temperatures are distinct and Fe–Cu ratio determines the alloy' properties. This study also was performed to show the Fe–Cu ratio influence on the thermal effect by differential scanning calorimetry (DSC) curves. Besides, the paper takes self-micro drill bits to prove that the selection of the alloy for bonding matrix in diamond bits should consider the drilling object. These results provide a guideline for using Fe–Co–Cu alloys as bonding matrix for geological diamond bits.

EXPERIMENTAL DETAILS

Three types of Fe–Co–Cu pre-alloyed powders were prepared by the co-precipitation method. Every element were weighted by mass ratio listed in Table 1 and dissolved into deionized water to form $\text{FeCl}_2 \cdot 4\text{H}_2\text{O}$, $\text{CoCl}_2 \cdot 6\text{H}_2\text{O}$ and $\text{CuCl}_2 \cdot 2\text{H}_2\text{O}$. The concentration of the solution was 1.0 mol/L. Subsequently, the as-prepared solution was mixed with 1.0 mol/L oxalic acid solution (1:1 ratio) and added into the reaction vessel at the same flow rate. In this reaction, the synthesis temperature is controlled to be 50 °C, with a pH of 2.0 adjusted by adding ammonia, and a reaction time of 20 min. After precipitating for 2 h, the Fe–Co–Cu compound oxalate precipitate was obtained. After filtering, washing, calcining and reducing, the pre-alloyed powders were formed.

* Hereinafter, the composition is given in wt %.

Table 1. Compositions of the pre-alloyed powders

Samples	Fe, wt %	Cu, wt %	Co, wt %
A	25	60	15
B	45	40	15
C	65	20	15

Based on the theoretical densities of the alloys and the volume of the graphite mold, three powders were weighted and then sintered in the vacuum hot press sintering furnace. In the sintering process, the vacuum level was under 0.1 Pa, the pressure was 54 MPa, sintering temperatures were 700, 750, 800, 850, 900 °C, respectively, and the sintering time was 6 min. The dimensions of sintering samples were 30×12×6 mm.

Three point bend tests were employed to determine the flexural strengths of the matrix. The span between the bottom pins was 25 mm. Five samples per composition were processed to obtain averaged values. Hardness testing was carried out using a TH300 Rockwell hardness tester, with the averaged values of 10 measurements. Using the drainage method, the densities of the matrix was measured and the relative densities were calculated based on the measured densities and theoretical density ratios.

Phase analysis was carried out using a D/max-Ra10 X-Ray Diffractometer. Microstructure analysis was performed using a JSM-6700F scanning electron microscope (SEM). Thermal properties were obtained by Differential Thermal Analysis Method. By testing the three point bending performance of the samples containing 29 wt % diamond (40/45 size), diamond holding strength was calculated according to

$$\sigma = \frac{M_i - M_d}{M_i} \cdot 100, \quad (1)$$

where M_i and M_d are the blank matrix and matrix contained diamond respectively.

Home-made micro diamond bits were used to measure the practical drill effect of powders. The rock used in the experiments was consisted of 30 wt % quartz, 55 wt % potassium feldspar and 15 wt % biotite, which belonged to the medium to hard formation and the drillability is seven. The dimension of the self-bit was 8 mm in diameter, 10 mm in height shown in Fig. 1. The height contained two parts, which were 6 mm long working layer contained diamond used to drill the rock and 4mm long welding layer for welding the micro bits to the steel body. Subsequently, the diamonds in size half 35/40 and half 40/45 by 8 wt % were added into the working layer and the bits were melt to the steel body. By measuring the drilling depth and bit wear height in the same time, the drill efficiency and theory service life were obtained. Considering that the experiment should be close to the real drilling condition, a matrix formula was designed aiming at this rock. Every ingredient was listed at Table 2. The formula A contained was No. 1, B was 2 and C was 3, respectively.

Table 2. Metal bond formula for medium to hard formation

Element	WC	A, B or C	Ni	Mn	CuSn ₁₅ Zn
wt %	25	50	10	5	10

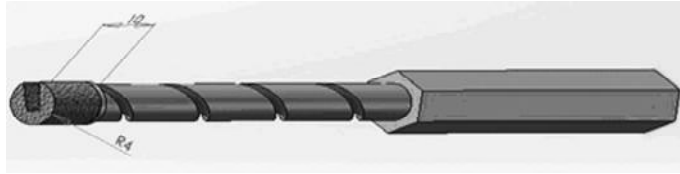


Fig. 1. Self-made micro diamond bit.

RESULTS AND DISCUSSION

Powders' structure

Figure 2 shows the X-ray diffraction (XRD) patterns of the Fe–Co–Cu powders with different Fe–Cu compositions. Co_3Fe_7 , $\text{CoFe}_{15.7}$ and FeCu_4 solid solutions presence are observed for all alloys. When Cu is reduced, Fe content is added, forming lower Fe–Cu solid solutions. This is observed with the reduction of relative intensities for associated peaks. It is noted that the peak at $2\theta = 74.22^\circ$ nearly disappears for high Fe content samples. However, the peak intensities for Fe and Cu also are influenced significantly by the Fe–Cu compositions [20–21]. The formation of solid solution is the key for explaining the hardness improvement in Fe–Cu–Co alloys in [21] should be doubted. The content of Fe and Co are basic influence factor. Some works are expected to found the quantity of the solid solutions, but this is still an open field and needs specific study. Peaks for elemental Co are not observed in Fig. 2, because Co forms solid solutions with Fe, which lead to the Co–Fe alloy phases appearing in Fig. 2.

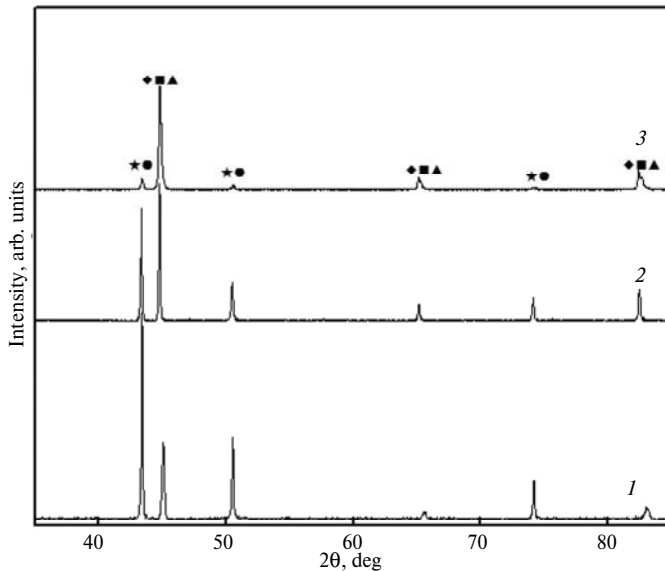


Fig. 2. XRD patterns of the three pre-alloyed powders: A (1), B (2), C (3) powders; Fe (♦), Cu (*), Co_3Fe_7 (■), $\text{CoFe}_{15.7}$ (▲), FeCu_4 (●).

Effect of Fe–Cu proportion on the powders' microstructure

The microstructures of powders with different Fe–Cu compositions are shown in Fig. 3. It is found that all the shapes of three powders are irregular and particles connect with each other loosely, resulting in large specific surface areas. Therefore, higher sintering activities can be obtained and the sintering temperatures will be

reduced. On the other hand, it can be found that A powder has the thickest particle as the Fisher particle size is 9.2 μm compared with the B (8.7 μm) and C (5.2 μm). This is because the higher the Cu contained, the easier the precursor reduced. Moreover, the powder with higher Cu concentration has lower recrystallization temperature, leading to faster processes for recrystallization and grain growth. In a word, the particle size has a strong affinity with Cu content, the microstructure changes due to the Fe–Cu ratio.

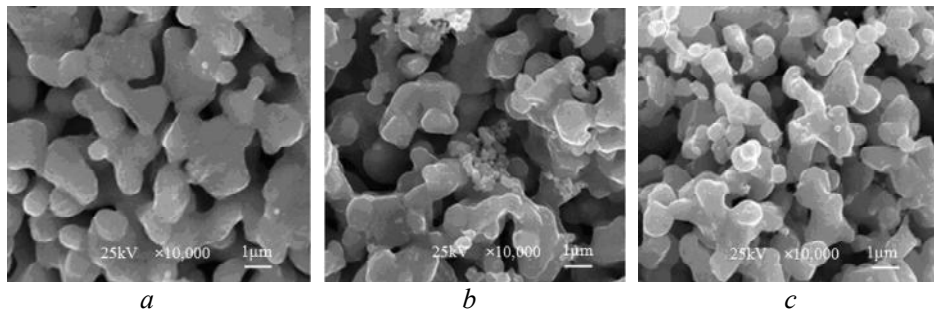


Fig. 3. SEM pictures of the three pre-alloyed powders: A (a), B (b), C (c) powders.

DSC curve of the powders

In Fig. 4, the DSC curves of different Fe–Cu proportion are shown. It can be found that no obvious heat changes appear below 980 °C but there are two endothermic peaks at about 980 and 1110 °C. In the binary systems of Fe–Cu, Fe–Co and Cu–Co, 980 °C is the $\alpha\text{Fe} \rightarrow \alpha\text{Co}$, γFe transformation temperature. Meanwhile, Fe–Cu, Co–Cu peritectic reactions occur at 1096 and 1112 °C, respectively. The A samples has lower Fe content so the endothermic peak at 980 °C is not present. The B samples exhibit the two peaks because Fe and Cu nearly have the same contents. C powder has low Cu composition so the peak at 1110 °C disappears. Figure 4 indicates that the simple substance of Fe, Co and Cu occupies a large proportion in the powder. The solid solutions appear in Fig. 2 have an important influence on the powder structures, but the ratio of three elements determines the powder's properties. When choosing the pre-alloyed powders as the metal bond used for diamond bits, the element composition should be a valuable reference.

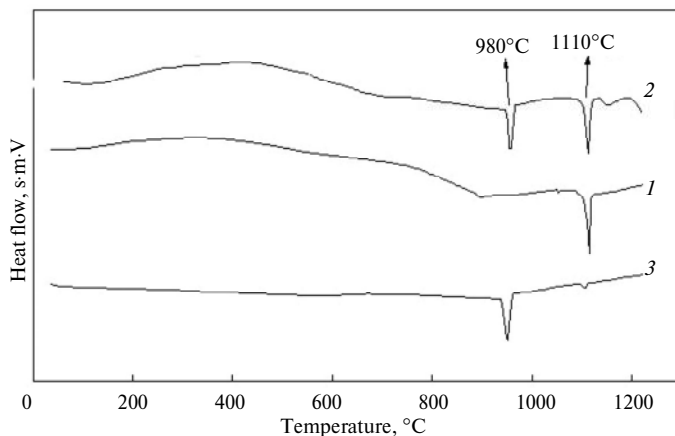


Fig. 4. DSC curves of the three pre-alloyed powders: A (1), B (2), C (3) powders.

Mechanical properties

Figure 5 present results of relative densities, three point bend strengths and hardnesses for powders sintered at different temperatures. It can be observed that the relative density increases with increasing temperature from Fig. 5, *a*. Meanwhile, with the increased Cu content, the relative density also increases. Based on the powder metallurgical theory, with the increased density the sintering process will carry out more sufficiently so the pore volume and pore number are reduced, which results in the higher relative density. When the samples are heated to a certain temperature, the elimination of the pore defect will slow down so the relative densities tend to be more stable. Cu element has a lower melting point, therefore, for the samples containing more Cu element, the sintering temperature will be reduced and densification process be promoted.

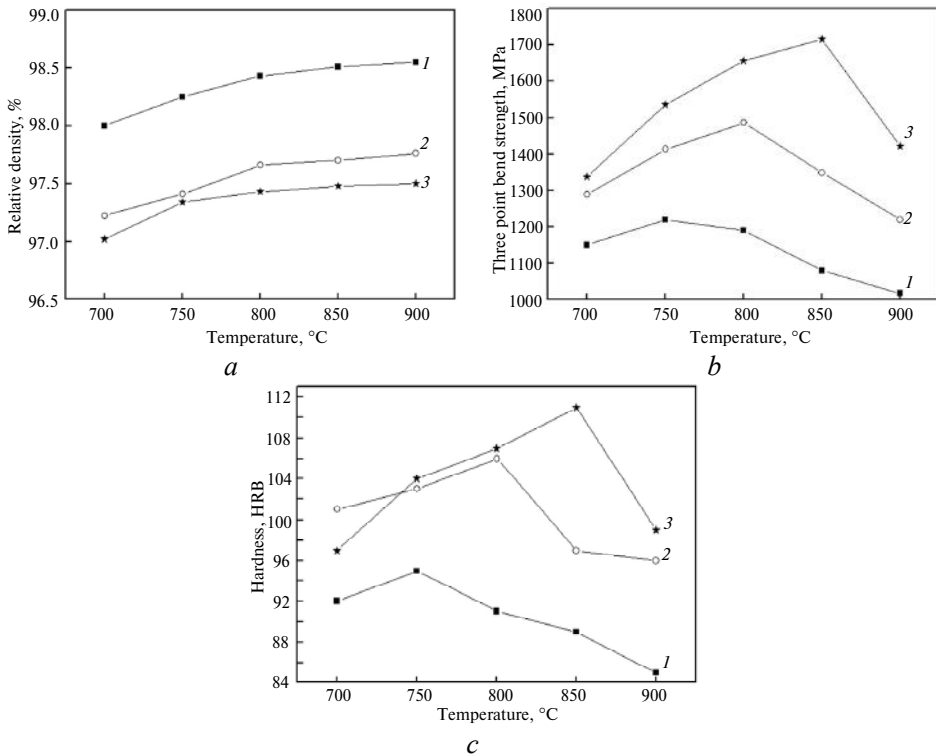


Fig. 5. Curves of the three matrix' mechanical properties sintered at different temperatures: relative density (*a*), three point bend strength (*b*), hardness (*c*); A (1), B (2), C (3) samples.

Figure 5, *b* shows the relationship between the strengths of three kinds of samples and sintering temperatures. It can be found that the strength is correlated to the Fe–Cu ratio. Cu element inducing plastic deformation needs less stress, so the more Cu contained, the lower strength the sample has. On the other hand, it can be found that the samples' strengths vary with temperatures. The strengths of all the three kinds of samples increase with temperature but decreases when temperature reaches to a transition point. The strength of A sample reaches to its maximum at 750 °C and B sample at 800 °C, C sample at 850 °C. At a low temperature, the sintering process incomplete, but at a higher temperature the grain size is larger. According to the Hall-Petch formula

$$\sigma_y = \sigma_i + kd^{-\frac{1}{2}} \quad (2)$$

where σ_y , d , σ and k are the samples' strength, grain size and constants, respectively. Compared with B and C, the best sintering temperature of A is the 750 °C which is the lowest. This can be explained by the Cu content. Cu element has a lower melting point so it can reduce the samples' sintering temperature with the higher Cu content. When Cu is reduced, Fe content is added, the sintering temperature shows increasing trend.

Figure 5, *c* shows the relationship between hardnesses and sintering temperatures. It can be observed that the change trend is similar to the strength. The hardness of C samples is higher than the others and the hardnesses for all the three types of samples increases at first then decreases as the sintering temperature rises. The reason is similar to the strength. Mechanical performances show that Fe–Cu ratio determines the properties of the powders.

Microstructure of sintered matrix

Figure 6 shows the microstructure of fracture surface on sintering specimens with different Fe–Cu ratios. A, B and C samples were sintered at 750, 800 and 750 °C as the samples have the perfect mechanical properties at the chosen temperature. It can be found that A sample has the typical character of dimple fracture due to the high Cu content. In A samples Cu is the main phase. Cu has better plastic deformation capacity so it was easier to formulate micro-cracks which interconnect with each other and grow to dimple. With the increased Fe composition, the strength rises. However, as the stress increase to some extent, cracks form and expand in the grains, resulting in trans-granular fracture. The more Fe contains, the more trans-granular fracture is formed. One can observe that B samples both have obvious dimple fracture and trans-granular fracture but C sample has typical character of trans-granular fracture in Fig. 6. It can be said that the Fe–Cu ratio determine the matrix' microstructure.

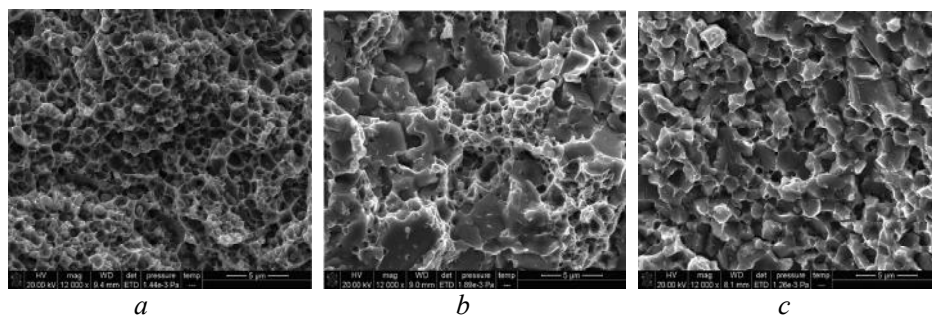


Fig. 6. Microstructures of the three sintered matrix: A (*a*), B (*b*), C (*c*) sample.

Diamond retention

Table 3 presents results of diamond retention of three powders and Fig. 7 shows the microstructure of fracture surface of 29 wt % diamond contained matrix. One can observe that C samples have the best retention. From the SEM images, it can be found that gaps exist between the matrix and diamond in all the three samples. The diamond retention is mainly based on the mechanical retention. Diamond in the A samples has a smoother interface and the gaps between matrix and particles are wider, because A samples have higher Cu content and Cu has weak wetting

ability to carbon materials so bond force in the interface is lower. Diamond in B samples erodes with the increased Fe content. Meanwhile, since in the works [1, 3, 5–8], by the methods of transmission electron microscopy and structural analysis, it has been established that carbides are formed at the interface of the contact of diamond particles with iron, as well as with certain compounds of transition metals, which significantly increases the retention of diamond particles by metallic matrix, mechanical and performance characteristics of the composite.

Table 3. Diamond intention of different samples

No.	Sintering temperature, °C	Strength of blank matrix, MPa	Strength of diamond contained matrix, MPa	Diamond intention, %
A	750	1220	830	31.97
B	800	1487	1180	20.65
C	850	1716	1450	15.5

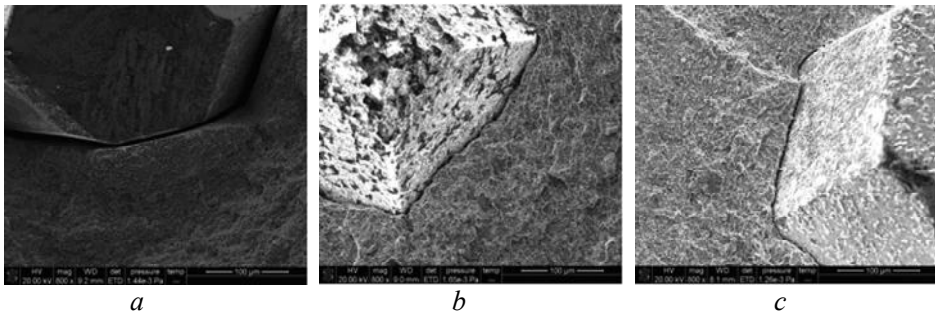


Fig. 7. Fracture images of diamond contained matrix: A (a), B (b), C (c) matrix.

Micro-drilling experiment

Table 4 presents results of application effects when used for drilling medium to hard formation (grade 7). It is found that the No. 1 sample has the best drilling efficiency (2.64 m/h) but the drilling life is the shortest (4449.44 mm). Drilling efficiency of No. 3 sample decreases, however, the drilling life almost doubles. The efficiency and life of No. 2 are both between those for the No. 1 and 3, but is close to No. 1. In No. 1 the matrix is soft due to the higher Cu content so the drilling cuttings have the strong grinding effect to the matrix, then the matrix wears more swiftly. Meanwhile, the diamond's drop-off and exposure accelerate, causing a higher drilling efficiency and a shorter drilling life. As the Fe content increases, the hardness and strength ascend and grinding effect of drilling cuttings on the matrix gets weaker. Simultaneously, the diamond's drop-off and exposure slow down so the drilling efficiency is lower but drilling life is longer. The drilling results show that Fe–Cu ratio determines the service performance of the powders.

CONCLUSIONS

In this work, the Fe–Co–Cu pre-alloyed powders were manufactured by co-precipitation method. Mechanical properties for powders sintered at different temperatures with different Fe–Cu ratios were investigated. Microstructures and diamond retention were studied. Micro drilling experiments were performed to examine the effect of Fe–Cu ratio on the powder performance. The main conclusions can be drawn as follows:

Solid solutions such as Co_3Fe_7 , $\text{CoFe}_{15.7}$, FeCu_4 are formed in all the powders with different Fe–Cu ratios. Microstructure varies with the Fe–Cu composition. The lower Cu composition, the finer the powder size.

Table 4. Micro drilling experiment results

Number	Drilling time, min	Bit wear height, mm	Drilling depth, mm	Drilling efficiency, m/h	Theoretical life, mm
1 (750 °C sintered)	30	1.78	1320	2.64	4449.44
2 (800 °C sintered)	30	1.22	1060	2.12	5213.1
3 (850 °C sintered)	30	0.57	915	1.83	9631.6

The suitable sintering temperature for the three Fe–Cu ratio powders is different and mechanical properties rely on the Fe–Cu ratio. As the Fe content increases, the mechanical properties are better.

Fe–Cu ratio has an important effect on the sintered matrix. The microstructure of the matrix with a high Cu content present the character of dimple fracture. As Fe content increases, the matrix show the character of trans-granular fracture. As the Fe content increases, the diamond retention is enhanced.

For the medium to hard formation 65 % Fe–20 % Cu–15 % Co powder has the best drilling performance. Elements match determines the service performance.

FUNDING

This work is supported by Guangxi Province Science Foundation for Youths (2017GXNSFBA198147) and Plan program of Scientific Research and Technical Development of Guilin in China (20180104-13)

Сплави Fe–Co–Cu використовують як металеві матриці нового покоління для геологічних алмазних бурів. У цій роботі синтезовано сплави Fe–Co–Cu з різним хімічним складом з використанням методу спільного осадження, які згодом спікали при різних температурах. Структурні, теплові властивості порошків і спечених матеріалів вивчали різними методами. Рентгенівські дифракційні дослідження показали, що тверді розчини цих сплавів утворюються під час спільного осадження. Мікроструктура попередньо легованих порошків показала, що процесу спікання сприяли неправильні форми, з'єднані між собою дрібні частинки, а також великі площі поверхні. Теплові ефекти попередньо легованих порошків досліджували за допомогою диференціальної скануючої калориметрії. Оптимальну температуру спікання для кожного попередньо легованого порошку було визначено механічним аналізом. Результати скануючого електронно-мікроскопічного дослідження показують, що співвідношення складу Fe і Cu суттєво вплинуло на мікроструктуру спечених матеріалів, а сплав 65 % Fe–20 % Cu–15 % Co мав найкраще покриття поверхні алмазних бурів. Виконання свердління для матеріалів з різними попередньо легованих порошків було перевірено експериментально мікробурінням. Ці результати свідчать про те, що сплав 65 % Fe–20 % Cu–15 % Co має оптимальні показники для застосування в геологічних алмазних бурях.

Ключові слова: попередньо легований порошок, спікання, метод спільного осадження, геологічний алмазний бур.

Сплавы Fe–Co–Cu используются как металлические матрицы нового поколения для геологических алмазных буров. В этой работе синтезированы сплавы Fe–Co–Cu с различными химическими составами с использованием метода совместного осаждения, которые впоследствии спекали при различных температурах. Структурные,

тепловые свойства порошков и спеченных материалов изучали разными методами. Рентгеновские дифракционные исследования показали, что твердые растворы этих сплавов образуются во время совместного осаждения. Микроструктура предварительно легированных порошков показала, что процессу спекания способствовали неправильные формы, соединенные между собой мелкие частицы, а также большие площади поверхности. Тепловые эффекты предварительно легированных порошков исследовали с помощью дифференциальной сканирующей калориметрии. Оптимальную температуру спекания для каждого предварительно легированного порошка определяли механическим анализом. Результаты сканирующего электронно-микроскопического исследования показывают, что соотношение состава Fe и Cu существенно повлияло на микроструктуру спеченных материалов, а сплав 65 % Fe–20 % Cu–15 % Co имел лучшее покрытие поверхности алмазных буров. Выполнение сверления для материалов из разных предварительно легированных порошков было проверено экспериментально микробурением. Эти результаты свидетельствуют о том, что сплав 65 % Fe–20 % Cu–15 % Co имеет оптимальные показатели для применения в геологических алмазных бурях.

Ключевые слова: предварительно легированный порошок, спекание, метод совместного осаждения, геологический алмазный бур.

1. Mechnyk V.A. Diamond–Fe–Cu–Ni–Sn composite materials with predictable stable characteristics. *Mater. Sci.* 2013. Vol. 48, no. 5. P. 591–600.
2. Bondarenko N.A., Zhukovsky A.N., Mechnik V.A. Analysis of the basic theories of sintering materials. 1. Sintering under isothermal and nonisothermal conditions (A review). *J. Superhard Mater.* 2005. Vol. 27, no. 6. P. 3–17.
3. Mechnik V.A. Production of diamond–(Fe–Cu–Ni–Sn) composites with high wear resistance. *Powder Metall. Met. Ceram.* 2014. Vol. 52, no. 9. P. 577–587.
4. Bondarenko M.O., Mechnik V.A., Suprun M.V. Special features of the shrinkage and its rate in the Cdiamond–Fe–Cu–Ni–Sn–CrB₂ system during hot pressing of presureess-sintered compacts. *J. Superhard Mater.* 2009. Vol. 31, no. 4. P. 232–240.
5. Mechnik V.A., Bondarenko N.A., Kuzin N.O., Lyashenko B.A. The role of the structure formation in forming the physicomechanical properties of composites of the diamond–(Fe–Cu–Ni–Sn) system. *J. Frict. Wear.* 2016. Vol. 37, no. 4. P. 377–384.
6. Kolodnits'kyi V.M., Bagirov O.E. On the structure formation of diamond-containing composites used in drilling and stone-working tools (A review). *J. Superhard Mater.* 2017. Vol. 39, no. 1. P. 1–17.
7. Gevorkyan E., Mechnik V., Bondarenko N., Vovk R., Lytovchenko S., Chishkala V., Melnik O. Peculiarities of obtaining diamond–(Fe–Cu–Ni–Sn) composite materials by hot pressing. *Funct. Mater.* 2017. Vol. 24, no. 1. P. 31–45.
8. Novikov M.V., Mechnyk V.A., Bondarenko M.O., Lyashenko B.A., Kuzin M.O. Composite materials of diamond–(Co–Cu–Sn) system with improved mechanical characteristics. Part 1. The influence of hot re-pressing on the structure and properties of diamond–(Co–Cu–Sn) composite. *J. Superhard Mater.* 2015. Vol. 37, no. 6. P. 402–416.
9. Aleksandrov V.A., Alekseenko N.A., Mechnik V.A. Investigation of force and energy parameters of the cutting granite with diamond disk saws. *Sov. J. Superhard Mater.* 1984. Vol. 6, no. 6. P. 35–39.
10. Dutka V.A., Kolodnitskiy V.M., Mel'nychuk O.V., Zabolotnyj S.D. Mathematical model for thermal processes occurring in the interaction between rock destruction elements of drilling bits and rock mass. *Sverkhтвердые Materialy.* 2005. Vol. 27, no. 1. P. 67–77.
11. Aleksandrov V.A., Mechnik V.A. The effect of diamond heat conductivity and heat transfer coefficient upon contact temperature and wear of cutting discs. *J. Frict. Wear.* 1993. Vol. 14, no. 6. P. 1115–1117.
12. Aleksandrov V.A., Zhukovsky A.N., Mechnik V.A. Temperature and wear of inhomogeneous diamond wheel under convective heat transfer. Part 1. *J. Frict. Wear.* 1994. Vol. 15, no. 1. P. 27–35.
13. Zhukovskii A.N., Maistrenko A.L., Mechnik V.A., Bondarenko N.A. The stress–strain state of the bonding around the diamond grain exposed to normal and tangent loading components. Part 1. Model. *J. Frict. Wear.* 2002. Vol. 23, no. 3. P. 146–153.
14. Zhukovskii A.N., Maistrenko A.L., Mechnik V.A., Bondarenko N.A. Stress–strain state of the matrix around the diamond grain exposed to the normal and tangent loading components. Part 2. Analysis. *J. Frict. Wear.* 2002. Vol. 23, no. 4. P. 393–396.

15. Sveshnikov I.A., Kolodnitsky V.N. Optimization of the hard alloy cutter arrangement in the drilling bit body. *Sverkhtrudye Materialy*. 2006. Vol. 28, no 4. P. 70–75.
16. Xie D.L., Wan L., Song D.D., Qin H., Pan X., Lin F., Fang X. Low-temperature sintering of FeCoCu based pre-alloyed powder for diamond bits. *J. Wuhan Univ. Technol. Mater. Sci.* 2016. Vol. 31, no 5. P. 805–810.
17. Hsieh Y.Z., Lin S.T. Diamond tool bits with iron alloys as the binding matrices. *Mater. Chem. Phys.* 2001. Vol. 72, no. 2. P. 121–125.
18. Oliveira L.J. Use of PM Fe–Cu–SiC composites as bonding matrix for diamond tools. *Powder. Metall.* 2007. Vol. 50, no. 2. P. 148–152.
19. Sun Y.X., Tsai Y.T., Lin K.K. The influence of sintering parameters on the mechanical properties of vitrified bond diamond tools. *Mater. Des.* 2015. Vol. 80, no. 5. P. 89–98.
20. Palumbo M., Curiotto S., Battezzati L.A. Thermodynamic analysis of the stable and metastable Co–Cu and Co–Cu–Fe phase diagrams. *Calphad*. 2006. Vol. 30, no. 2. P. 171–178.
21. Shao W.Q., Chen S.O., Li D., Cao H.S., Zhang Y.C., Ge X.H. Prediction of densification during low heating rate sintering of microcrystalline alumina ceramics based on master sintering curve theory. *Mater. Proc. Report*. 2008. Vol. 23, no. 1. P. 19–22.

Received 23.05.18

Revised 06.03.19

Accepted 11.03.19